Effect of Earthquake Frequency Content on 3D Sloshing in Rectangular Tanks

Hamid Reza Mohammadi[1] and Mohammad Safi[2*]

1. M.Sc. Graduate, Department of Civil, Water and Environmental Engineering, Shahid Beheshti University, Tehran, Iran
2. Assistant Professor, Department of Civil, Water and Environmental Engineering, Shahid Beheshti University, Tehran, Iran,
* Corresponding Author; email: m_safi@sbu.ac.ir

Received: 11/01/2017
Accepted: 13/06/2018

ABSTRACT

Earthquake frequency content has a significant effect on sloshing wave amplitude and height in liquid storage tanks. In this paper, the finite element method had been used to obtain the three dimensional fluid-structure interaction response of the rectangular tanks to access the sloshing interference effects at the tank corners under various seismic input motions with different frequency contents. The flexibility of the tank wall as well as the structural and fluid damping have been taken into account to obtain more reliable and realistic results. It has also been shown that the 3D sloshing interference may increase the total wave height significantly at the corners of the tanks compared to the values presented in the design codes, which shows the maximum sloshing wave with much lower values and at a different location. It has been finally shown that the 3D sloshing effects relates to the ratio of the width and the length of the tank.

Keywords:
Fluid-structure interaction; Frequency content; 3D sloshing; Rectangular tanks; Finite element method

1. Introduction

Water tank as a major element in water infrastructure system has suffered a lot of damage during past earthquakes. The 1964 Alaska earthquake caused the first large-scale damage to concrete water tanks of modern design and initiated many investigations into the dynamic interaction characteristics of flexible containers [1]. Among these studies, several investigations were carried out to obtain the dynamic interaction response between the deformable wall in the tank and the liquid. These studies showed that the seismic response of a flexible wall tank might be substantially greater than that of a similarly rigid wall tank.

Numerous studies have been carried out on seismic behavior of ground-level cylindrical tanks. However, the conditions are not the same for underground tanks, rectangular tanks, and elevated tanks. Almost the entire major studies about this subject may be summarized as follows.

Hoskins and Jacobsen [2] presented the first report on analytical and experimental observations of rigid rectangular tanks under a horizontal earthquake excitation. Graham and Rodriguez [3] used a spring-mass analogy for the fluid in a rectangular container. Housner [4-5] proposed a widely used analytical model for calculation of the hydrodynamic pressures, which separates it into impulsive and convective components. In this formulation, fluid has been assumed incompressible, and the walls were assumed to be rigid. This method has been

adopted with some modifications in most of the current codes and standards, such as the American Concrete Institute code (ACI 350.3-06) [6]. Finally, Epstein [7] extended Housner's procedures in the sense of practical design rules.

Three degree of freedom model of the ground supported cylindrical tank was developed by Haroun [1], the application of which resulted in design charts used to estimate sloshing wave, impulsive and rigid masses. In addition, Haroun [8] presented an analytical method in the typical system of loadings in rectangular tanks. In his work, the hydrodynamic pressures were also calculated using the classical potential flow approach. The formulas of hydro-dynamic pressures only considered the rigid wall boundary condition and neglected the flexibility of the surrounding wall.

Kim et al. [9] further developed an analytical solution method and presented the response of flexible wall rectangular tanks under vertical excitation, but the flexibility of walls was not thoroughly considered in the liquid-structure inter-action. They also considered the dynamic behavior of three-dimensional rectangular flexible fluid containers using the Rayleigh-Ritz method.

Dogangun et al. [10] investigated the seismic response of water rectangular storage tanks using analytical finite element methods. The fluid was assumed to be linear-elastic, inviscid, and compressible. A displacement based fluid finite element method was employed and the effectiveness of the Lagrangian approach for seismic analysis of tanks and the effects of wall flexibility on their dynamic behavior were also investigated.

Koh et al. [11] directed a thorough research on the effect of the 3D restraint condition on the dynamic behavior of the rectangular tank using 3-D coupled Boundary Element-Finite Element Method (BEM-FEM). They also investigated the sloshing behavior of the externally excited rectangular tank and compared their outcome with experimental test result.

Chen and Kianoush [12] used the sequential method to obtain the hydrodynamic pressure in two-dimensional rectangular tanks including the effect of wall flexibility but ignoring the fluid sloshing. Besides, Kianoush and Chen [13] investigated the dynamic behavior of rectangular tanks subjected to vertical seismic vibrations in a 2D model. The importance of vertical component of earthquake on the overall response of tank-fluid system was also discussed. In addition, Kianoush et al. [14] introduced a new method for seismic analysis of rectangular containers in 2D space where the effects of both impulsive and convective components were included in time domain.

Livaoglu [15] evaluated the dynamic behavior of fluid-rectangular tank-foundation system with a simplified seismic response analysis procedure. In this procedure, interaction effects were presented by Housner's two mass approximations for fluid, and the cone model used to consider the effect of soil foundation system. Recent studies has also been done on laboratory model of rectangular tanks under 3D excitation such as Hosseini and Alizadeh [16], and Hosseini et al. [17].

In the present study, the dynamic interaction response of three-dimensional rectangular concrete water tanks has been investigated using the displacement based finite element with direct integration method. The study includes the comparison of the effect of rigid and flexible walls under horizontal component of earthquake with various frequency contents. The parametric study used rectangular tanks with different geometries and length to height ratios. These models has been used to investigate three-dimensional sloshing at rectangular tank corners considering various characteristics of seismic input motion.

2. Fluid-Structure Interaction in Rectangular Tanks

2.1. Displacement Based Formulation of Fluid Finite Element

One of the most efficient methods that includes the effect of sloshing in computational fluid analysis is the displacement-based formulation. In order to implement this method, the shear modulus of the fluid is set to zero and the bulk modulus is directly used for constitutive relation of stress and strain. Such formulation can only be used where there is no flow or the fluid is contained inside a tank. The stress-strain relationship that defines the stiffness formulation can be shown as:

$$\begin{Bmatrix}\varepsilon_{bulk}\\ \gamma_{xy}\\ \gamma_{yz}\\ \gamma_{xz}\\ R_x\\ R_y\\ R_z\end{Bmatrix}=\begin{bmatrix}1/K & 0 & 0 & 0 & 0 & 0 & 0\\ 0 & 1/S & 0 & 0 & 0 & 0 & 0\\ 0 & 0 & 1/S & 0 & 0 & 0 & 0\\ 0 & 0 & 0 & 1/S & 0 & 0 & 0\\ 0 & 0 & 0 & 0 & 1/B & 0 & 0\\ 0 & 0 & 0 & 0 & 0 & 1/B & 0\\ 0 & 0 & 0 & 0 & 0 & 0 & 1/B\end{bmatrix}\times\begin{Bmatrix}P\\ \tau_{xy}\\ \tau_{yz}\\ \tau_{xz}\\ M_x\\ M_y\\ M_z\end{Bmatrix} \quad (1)$$

where ε_{bulk} is defined as $\varepsilon_{bulk}=\frac{\partial u}{\partial x}+\frac{\partial v}{\partial y}+\frac{\partial w}{\partial z}$ and the other parameters are as follows:

K = Fluid bulk modulus

P = Fluid pressure

γ = Shear strain

$S = K \times 10^{-9}$ (little arbitrary numbers are given to element for the stability in shear)

τ = Shear stress

R_i = Rotation about i axes

$B = K \times 10^{-9}$ (little arbitrary numbers are given to element for the stability in Rotate)

M_i = Torsional moment about i axes

In this formulation, the damping matrix that relates the strain rate and stress can be defined as:

$$\begin{Bmatrix}\dot{\varepsilon}_{bulk}\\ \dot{\gamma}_{xy}\\ \dot{\gamma}_{yz}\\ \dot{\gamma}_{xz}\\ \dot{R}_x\\ \dot{R}_y\\ \dot{R}_z\end{Bmatrix}=\begin{bmatrix}0 & 0 & 0 & 0 & 0 & 0 & 0\\ 0 & 1/\eta & 0 & 0 & 0 & 0 & 0\\ 0 & 0 & 1/\eta & 0 & 0 & 0 & 0\\ 0 & 0 & 0 & 1/\eta & 0 & 0 & 0\\ 0 & 0 & 0 & 0 & 1/C & 0 & 0\\ 0 & 0 & 0 & 0 & 0 & 1/C & 0\\ 0 & 0 & 0 & 0 & 0 & 0 & 1/C\end{bmatrix}\times\begin{Bmatrix}P\\ \tau_{xy}\\ \tau_{yz}\\ \tau_{xz}\\ M_x\\ M_y\\ M_z\end{Bmatrix} \quad (2)$$

where η represents the viscosity of fluid and is defined as $C = 0.00001\eta$.

This element assumes the mass matrix as lumped mass. In order to satisfy the boundary condition on the fluid surface, a spring element with the equivalent stiffness has been assigned to each node element at this boundary. The corresponding stiffness can be obtained using Equation (3).

$$K_S = \rho_l A_f (g_x C_x + g_y C_y + g_z C_z) \quad (3)$$

where ρ_l, A_f, g_i, C_i represent fluid density, area of the face element, acceleration along direction i, and the components normal to the face of the element, respectively. These elements have only been used at the fluid free surface.

3. Three-Dimensional Sloshing Analysis

3.1. Specifications of the Models

A schematic configuration of a rectangular concrete tank, which is more common in design codes and practice has been shown in Figure (1). In this study, two different configurations associated with shallow and tall tanks have been investigated in both two and three-dimensional spaces. In this

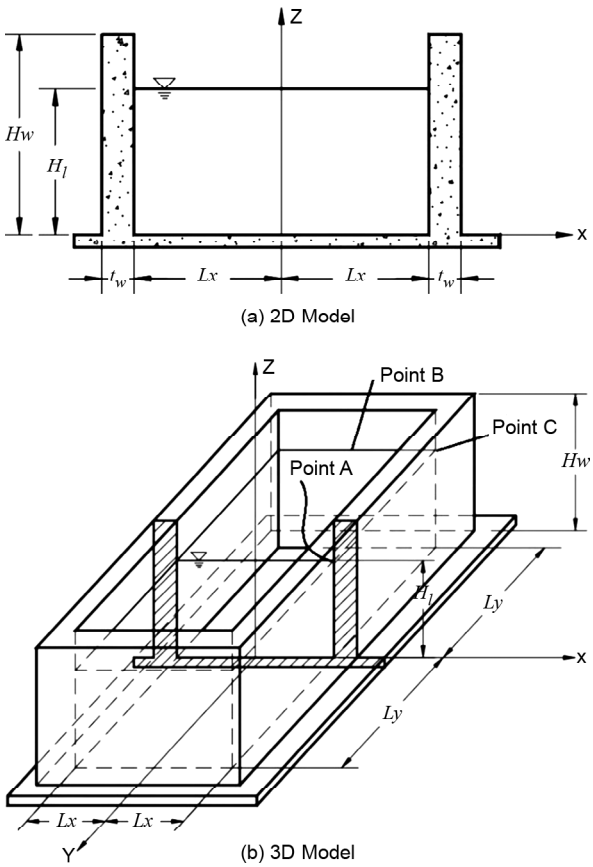

Figure 1. Schematic model of the rectangular tanks.

figure, points A, B and C show the locations where the results of sloshing have been presented.

A unit length strip at the middle of the tank along the longitudinal direction has been used to form the two-dimensional model of the system. For three-dimensional modelling, the tank has been assumed as a symmetric structure with four flexible walls. It has also been assumed that the tank is fixed or anchored to the base and the effect of uplift and the soil-structure interaction has been neglected.

In Table (1), the characteristics of the two groups of tank models used in this study have been defined. Shallow and tall tanks have 5.5 and 11 meters fluid height (H_L), respectively. The same geometry have been used in previous investigations done by Ghaemmaghami and Kianoush [18], Kim et al. [9] and Chen and Kianoush [12]. Each of the following groups has four tanks with different dimensions.

In all the simulations, water and concrete materials have been considered with the following properties:

Concrete Structure:

$$E_c = 21\ GPa$$
$$v_c = 0.17$$
$$\rho_c = 2400\ Kg/m^3$$

Water:

$$\rho_l = 1000\ Kg/m^3$$
$$B_l = 2.10\ GPa$$

where $E_c, \rho_c,$ and v_c are modulus of elasticity, density and Poisson's ratio of the tank structure respectively. B_l and ρ_l are bulk modulus and density of the fluid domain.

It should be noted that fluid elements at a boundary are not attached directly to structural elements; however, they have separate, coincident nodes that are coupled only in the direction normal to the interface. Couplings have been applied at the wet surface of the wall as well as the bottom of the tank.

Tank walls have been modelled as Iso-parametric solid elements with eight nodes, each with three degrees of freedom (DOF). The liquid domain has also been modelled by three-dimensional Iso-parametric eight nodes fluid elements having three DOF at each node.

In addition, in order to construct the two-dimensional model, the structure has been simulated using four node elements with two translations DOF at each node forming a plane strain behavior. In order to obtain more accurate results in 2D plane strain models, fluid domain were modelled with both four node Iso-parametric element as well as the four node acoustic element. The four node acoustic element has pressure DOF at each node. Acoustic element has been used to calculate the resulting forces and moments, as well as the hydrodynamic pressure distribution along the height of the walls. On the other hand, Iso-parametric elements have been employed to estimate the sloshing height.

Table 1. Configuration and geometry of the tanks used in this study.

	Model Name	$2L_x$ (m)	$2L_y$ (m)	H_w (m)	t_w (m)
Shallow Tank H_L = 5.5 (m)	SX20Y40	20	40	6	0.6
	SX20Y60	20	60	6	0.6
	SX30Y60	30	60	6	0.6
	SX40Y40	40	40	6	0.6
Tall Tank H_L = 11 (m)	TX20Y40	20	40	12	1.2
	TX20Y60	20	60	12	1.2
	TX30Y60	30	60	12	1.2
	TX40Y40	40	40	12	1.2

3.2. Selection of Seismic Input Accelerograms

One of the important factors in dynamic time history analysis is the selection of input earthquake records. The response of fluid-structure system strongly depends on the characteristics of these earthquakes. This issue will be discussed later in more detail. Table (2) presents the characteristics of earthquake records used in this study. The criteria for selection of earthquake records include the frequency content, predominant period of earthquake and power spectral density function (PSD).

Appropriate indicators to determine the frequency content of ground motion is ratio of peak ground acceleration (PGA) to peak ground velocity (PGV). Accordingly, earthquake ground motion in accordance with the frequency content can be divided into three categories as follows:

- If $\frac{PGA}{PGV} > 1.2$, earthquake will be considered as high frequency content.
- If $0.8 < \frac{PGA}{PGV} < 1.2$, earthquake will be considered as intermediate frequency content.

Table 2. Summary of Information and parameters of ground motions used in this study.

ID No.	Earthquake				Site Data	Site-Source Distance (km)	Predominant Period (sec)	Type of Frequency Content
	Name	Year	M	Record Seq. No.	V_s (m/sec)	Joyner-Boore	T	
1	Loma Prieta	1989	6.93	791	608	33.9	0.74	Low
2	Landers	1992	7.28	848	353	19.7	0.34	Intermediate
3	Loma Prieta	1989	6.93	745	423	71.3	0.4	Intermediate
4	San Fernando	1971	6.61	91	487	61.7	0.24	High

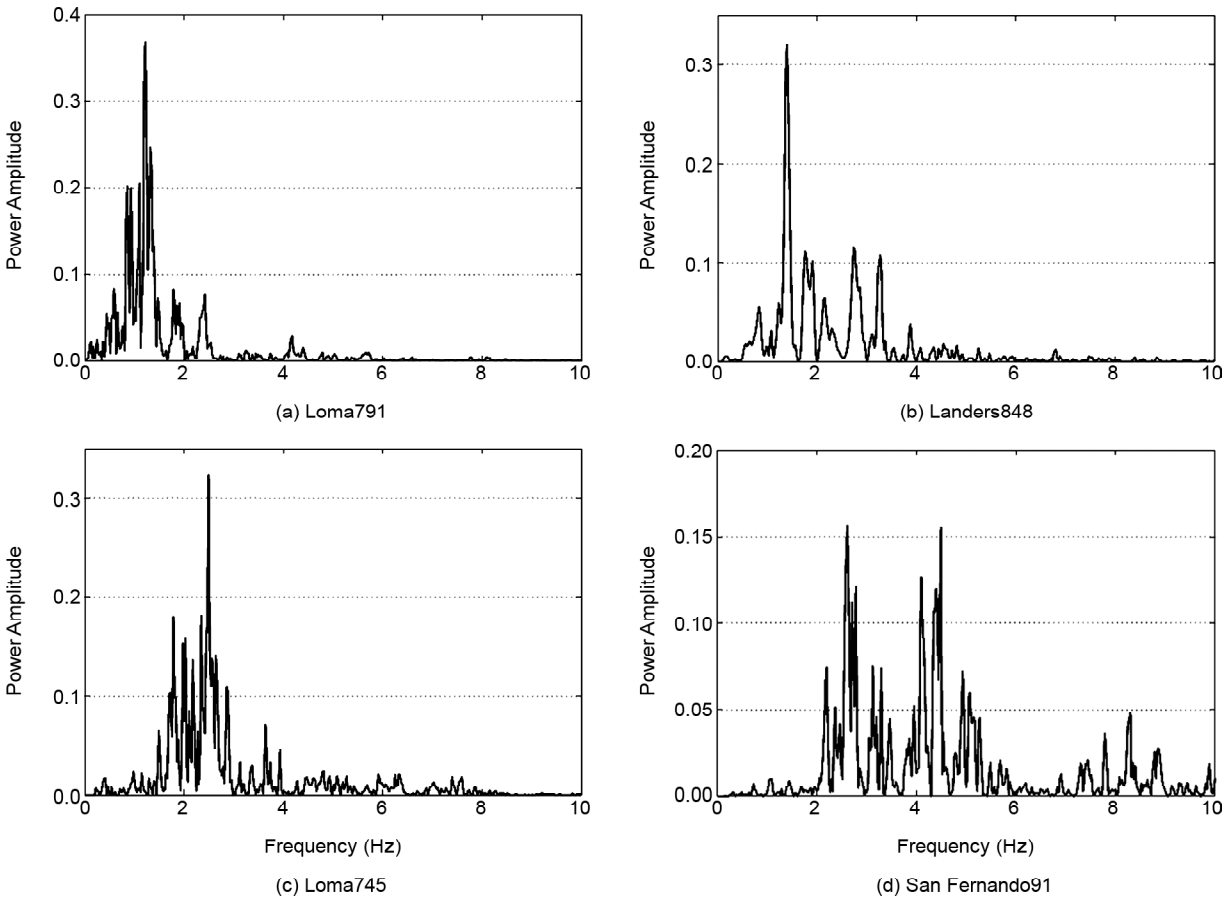

Figure 2. Power spectral density functions (PSD) of ground motions.

- If $\frac{PGA}{PGV} < 0.8$, earthquake will be considered as low frequency content.

According to this classification, Loma791, Landers848, Loma745 and San Fernando91 placed in categories of low, intermediate and high frequency content. In addition, two horizontal components of the earthquake has been applied simultaneously for three-dimensional analyses.

Selected records have the following properties:

1. The minimum magnitude of more than six.
2. The shortest horizontal distance to Joyner-Boore distance is equal to or more than 20 km. It should be noted that, in FEMA P695 [19] the boundary between near-field and far-field earthquakes has been defined to be around 10 km from the source to site.
3. The selected records corresponds to the shear wave velocity of soil in the range of 375 m/s $\leq V_{S30} \leq$ 750 m/s.
4. Minimum significant duration of each record is 10 sec.

In Figure (2), the power spectral density function (PSD) of time history records have been shown. This spectrum presents the energy distribution at different frequencies and demonstrates the concentration of ground motion energy in the mass center of these functions. Based on these functions, the maximum structural response is obtained when the predominant natural frequency tends to the mass center of the PSD function.

3.3. Verification Process

Several factors affect the fluid-structures interaction response. Among these factors, the most important ones are structural and fluid damping and flexibility of surrounding wall. In this section, the verification of the models has been performed by comparing the results with the previous studies. The comparison of the results with mathematical models have also been done to validate their accuracy.

Verification model has been used that included structural damping [11]. The dimensions and characteristics of the materials used for this study are:

$t_w = 1\ m$ $\quad \rho_c = 2400 Kg/m^3$

$L_x = 10\ m$ $\quad \rho_l = 1000 Kg/m^3$

$L_y = 25\ m$ $\quad E_c = 21 GPa$

$H_l = 9\ m$ $\quad v = 0.17$

$H_w = 10\ m$

The first 10 seconds of El Centro earthquake scaled to 0.4 g has been used for input motion. The tank has been assumed to be fixed to the ground with 3 percent structural damping. Flexible boundary condition for tank walls has been assumed and impulsive component of hydrodynamic pressure distribution were obtained as shown in Figure (3). Again there is an acceptable satisfaction between the results of the two simulations.

Sloshing height were calculated at free surface and in the middle of the tank. The results were compared with works done by Koh et al. [11], Hashemi et al. [20], Ghaemmaghami and Kianoush [18] (Figure 4). The figure shows a good compatibility between the results by the two approach namely the boundary-finite element and the finite element. It can be seen from the results that the boundary element-finite element method presents less sloshing response and less accuracy at the peak points compared to the finite element approach.

4. Investigation of 3D Sloshing

4.1. Modal Analysis

In order to check the general dynamic characteristics of the structures as well as the calculation of the damping coefficients for Rayleigh α, β, it is necessary to perform modal analysis. The natural period of the first mode of sloshing and also the impulsive mode, as well as the mass ratio corresponding to those modes have been calculated using FEM and compared to values presented in ACI 350.3-06 [6]. The results have been summarized in Table (3) for 3D models of shallow and tall tanks. The ACI 350.3-06 [6] formulation for calculating these frequencies is:

$$f_c = \frac{1}{2\pi}\sqrt{\frac{3.16(g)\tanh\left[3.16\left(H_L/L\right)\right]}{L}}, \qquad T_c = \frac{1}{f_c} \tag{4}$$

ACI 350.3-06 defines the two equivalent weight components of accelerating liquid by adopting the Houser's equation [5], and given as:

$$\frac{W_c}{W_L} = 0.264\left(L/H_L\right)\tanh\left[3.16\left(H_L/L\right)\right] \tag{5}$$

$$\frac{W_i}{W_L} = \frac{\tanh\left[0.866\left(L/H_L\right)\right]}{0.866\left(L/H_L\right)} \tag{6}$$

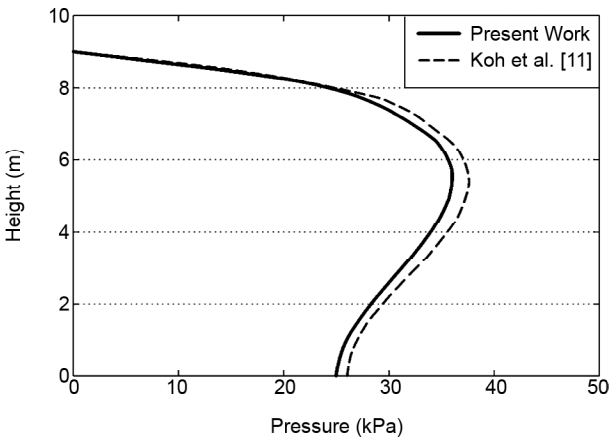

Figure 3. Comparison of pressure distribution along height of flexible wall tank.

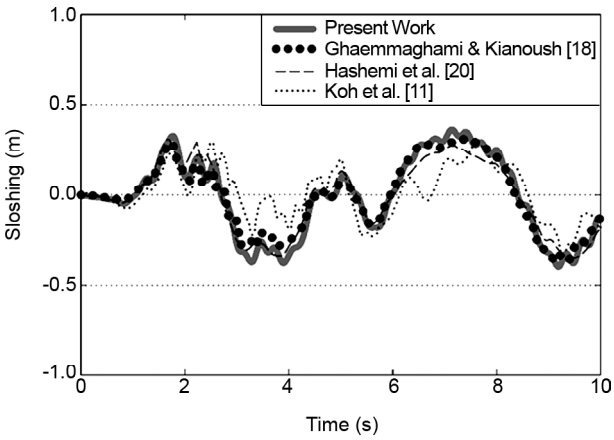

Figure 4. Comparison of time history of sloshing height in the middle section of the tank parallel to wall length.

Table 3. Comparison of periods and mass ratios of the present study with the ACI 350.3-06 code for three-dimensional model along the tank width (X-dir).

	Model Name	FEM				Code ACI			
		Time Period (s)		Mass Ratio		Time Period (s)		Mass Ratio	
		T_i	T_c	m_i/m	m_c/m	T_i	T_c	m_i/m	m_c/m
Shallow Tank H_L = 5.5 (m)	SX20Y40	0.16	6.07	0.16	0.42	0.11	6.03	0.32	0.67
	SX20Y60	0.17	6.07	0.16	0.44	0.11	6.03	0.32	0.67
	SX30Y60	0.17	8.60	0.12	0.52	0.11	8.56	0.21	0.75
	SX40Y40	0.16	11.22	0.08	0.61	0.11	11.16	0.16	0.78
Tall tank H_L = 11 (m)	TX20Y40	0.26	5.32	0.28	0.29	0.18	5.21	0.58	0.45
	TX20Y60	0.28	5.32	0.28	0.27	0.18	5.21	0.58	0.45
	TX30Y60	0.31	6.92	0.20	0.39	0.18	6.82	0.42	0.59
	TX40Y40	0.26	8.60	0.18	0.49	0.19	8.53	0.32	0.67

Table 4. The maximum sloshing height in shallow three-dimensional tanks.

			Model Name			
		Point (cm)	SX20Y40	SX20Y60	SX30Y60	SX40Y40
Shallow Tank	Rigid	A	32.5	33.1	25	18.7
		B	17.2	12.5	12.5	20.9
		C	42.5	26.7	31.4	14.1
	Flexible	A	32.9	33.6	25.3	19.2
		B	17.2	12.5	12.8	20.9
		C	42.6	26.8	31.5	14.3

Table 5. The maximum sloshing height in tall three-dimensional tanks.

			Model Name			
		Point (cm)	SX20Y40	SX20Y60	SX30Y60	SX40Y40
Tall Tank	Rigid	A	48.7	48.8	40.7	30.4
		B	34.1	21.7	22.2	34.5
		C	56.1	41.1	56.1	17.3
	Flexible	A	48.9	49.1	41.2	31.2
		B	34	21.1	22.5	32.5
		C	55.7	40.7	56.6	17.9

where W_i and W_c are the equivalent weight of the impulsive and convective component of the liquid, respectively.

As shown in Table (3) the predominant period of convective mode has been obtained with very little difference in both the finite element method and ACI 350.3-06 [6] as the linearized wave equation has been used in both methods. In addition, the predominant period of convective mode in the finite element method has always larger values than of the ACI 350.3-06 [6]. The main reason for this issue is that the flexible boundary condition has been considered for the finite element models, resulting an increase in the predominant period of convective mode. On the other hand, the difference between frequencies of the wall and the convective mode in this case is not noticeable, because the frequency of the tank structure is much higher than the fluid convective frequency.

4.2. Effect of Wall Flexibility on 3D Sloshing Response

Due to the influence of various parameters on sloshing response at critical points of the rectangular tanks such as the flexibility of the walls, three-dimensional geometry and dimensions of the tank, a comparative study has been performed in this section. Horizontal component of Landers848 earthquake record with intermediate frequency content has been used for this purpose. The maximum sloshing response has been shown in Tables (4) and (5) for three-dimensional models.

Based on the obtained results, sloshing height has been reduced by the increase in the length of the tank wall because the predominant period of the sloshing mode has been decreased and placed away from the predominant period of the earthquake. Hence, the sloshing height has been decreased in the tanks considering the predominant period of

Landers848 record equal to 0.34 sec. In addition, the sloshing height has been increased in the tanks with the same dimension in the plan by increasing the height of fluid from 5.5 to 11.0 meters as the predominant period of the sloshing will be decreased and become closer to the predominant period of the input earthquake. It should be noted that the sloshing will increase by increasing the fluid height, but the ratio of the maximum sloshing height to the height of fluid $\left(\delta_{max}/H_L\right)$ in the shallow tank remains higher compared to the tall tank (Figure 5).

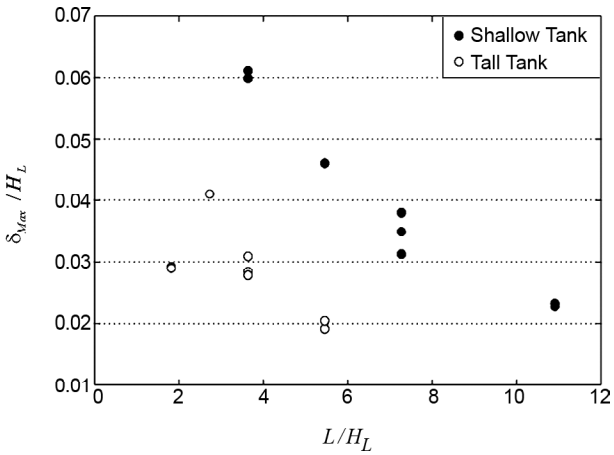

Figure 5. A comparison of the relative sloshing in shallow and tall tank.

In general, flexible boundary condition increased the height of sloshing, but not very significantly. This is due to the fact that the frequency of tank structures is very different from the frequency of the sloshing mode. In other words, the effect of wall flexibility is not significant on the response of the sloshing, because the frequency of tank structure is much higher than the frequency of the sloshing.

The sloshing height has been decreased in three-dimensional models compared with two-dimensional models under Landers848 earthquake record. In addition, the difference between two and three-dimensional models have been decreased when the ratio $\left(B/L\right)$ (B represent inside dimension of a rectangular tank perpendicular to the direction of the ground motion, and L represent the inside dimension of a rectangular tank parallel to the direction of the ground motion) increased. Thus, for these models, the two-dimensional model can be used with acceptable accuracy.

4.3. Effect of Earthquake Frequency Content on Sloshing Response

In this section, the effect of earthquake frequency content on the three-dimensional sloshing response of rectangular tanks has been investigated. Two models named as TX30Y60 and SX30Y60 have been used from Table (1) with similar plan but different fluid heights equal to 11.0 and 5.5 meters respectively and with flexible boundary conditions.

Four earthquake records with the same transversal and longitudinal PGA have been used as input motion namely Loma791, Landers848, Loma745 and San Fernando91. 25 seconds of the main shock of each earthquake has been used as time history input load. The Loma791 record with predominant period of 0.74 seconds is a low frequency earthquake. On the other hand, Loma745 and Landers848 records with predominant frequency of 0.40 and 0.34 seconds are in the range of intermediate frequency earthquakes. Finally, the San Fernando91 record with predominant frequency of 0.24 seconds lays in the range of high frequency earthquakes.

Using the characteristics of spectral density function to show the energy distribution with respect to frequency (Figure 2), it can be seen that the Loma791 earthquake, with the lowest mass center within the other records, would result in greater dynamic response of the structure.

In Figures (6) and (7), the maximum sloshing height has been shown at points A and B, respectively. The peak ground acceleration has identical value in all four records, but because the mass center of the power spectral density function in the Loma791 record has lower frequency value than the other records, the maximum sloshing height has been obtained for this record. On the other hand, as the predominant period of the Loma791 earthquake record is closer to the predominant period of the sloshing mode in comparison with other records, higher sloshing height has been obtained compared to the three others. For San Fernando91 record, the mass center of the power spectral density function is in the range of higher frequencies with bigger difference with the sloshing frequency, a smaller sloshing response has been obtained.

The above concept have been developed to investigate the effect of the earthquake characteristics on the interference of the waves in the tank

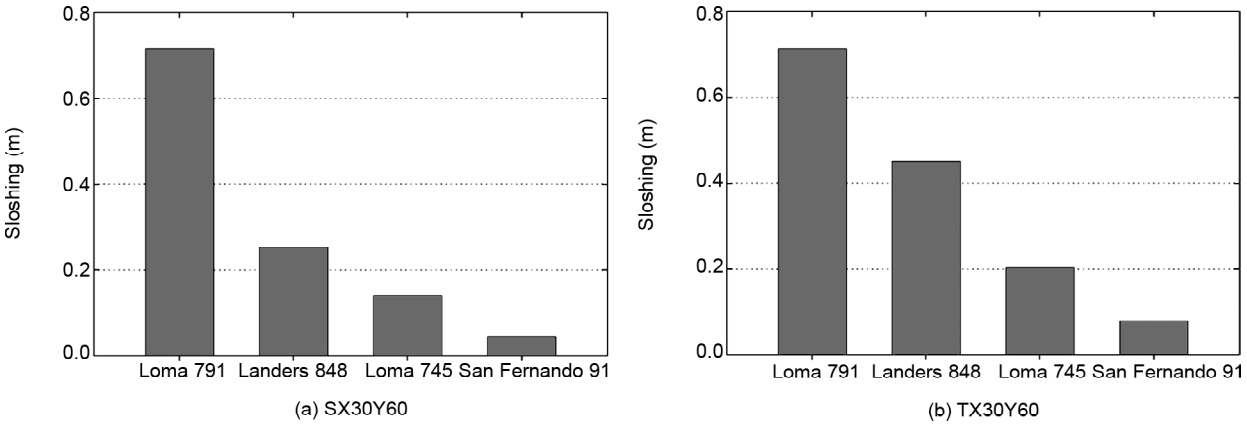

Figure 6. Maximum sloshing height at point A.

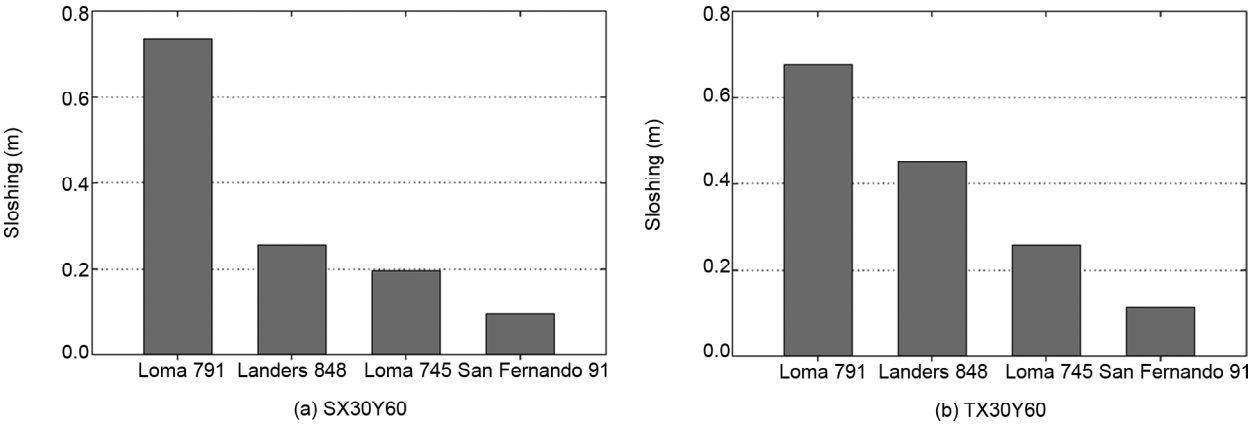

Figure 7. Maximum sloshing height at point B.

corners due to the sloshing. For this purpose, two models SX30Y60 and TX30Y60 have been considered under earthquake records with different frequency content. In Figure (8), the responses of sloshing have been shown under Loma791 record. In the model name SX30Y60, the maximum positive sloshing height at point C has been obtained in 19.02 sec., equal to 78.9 cm. At the same time, the sloshing height at points A and B is equal to 52.7, 26.1 centimetres, respectively. Since the heights of sloshing at this time have the same phase, the resulting wave has been called as constructive wave. Sloshing height at point C has been increased about 49.7 and 202 percent in comparison with points A and B, respectively.

The maximum sloshing height has been occurred in 15.10 sec. of analysis at point C with the value of 11.3, 863 percent more than points A, B in the same time. In addition, the maximum sloshing height at point C has been determined at time 1.62 sec. of the analysis and equal to 33.7 cm. At this time, the corresponding height at points A, B reach to 16.1 and 17.6 cm, respectively. The waves have the same phase again and form a constructive wave. Thus, the sloshing height at point C has been increased about 109 and 91.4 percent in comparison with points A and B, respectively.

In order to investigate the maximum effect of wave superposition at the corner point of the fluid tend the time history response of the sloshing wave has been shown in Figure (8) for points A, B and C. Based on the results obtained from Figure (8b) regarding the sloshing response in model TX30Y60, considering the increase of the fluid depth from 5.5 to 11 meters, the sloshing wave height has also been increased. This wave height reaches to 46.0 cm at time 1.64 sec. for point C. At the same time for points A and B, the sloshing wave height has been obtained equal to 21.2 and 24.7 respectively, which shows 117 and 86.2 percent smaller values compared to the corner point C. This shows the effect of superposition of the sloshing waves at the tank corner similar to the results shown for SX30Y60 model at time 1.62 sec. of the response.

The maximum sloshing height at point A has been determined at the time 9.54 sec. equal to 71.4 cm. At this time, the corresponding height at points C and B reach to 60.5 and 10.4 respectively. The absolute maximum response for point C has been happened at time 4.38 sec. with the sloshing height of 63.7 that shows 8.3 and 785 percent greater value compared to points A and B at the middle span of the wall. Figure (9) shows the interference of the waves at the corner of TX30Y60 tank under Loma791 earthquake.

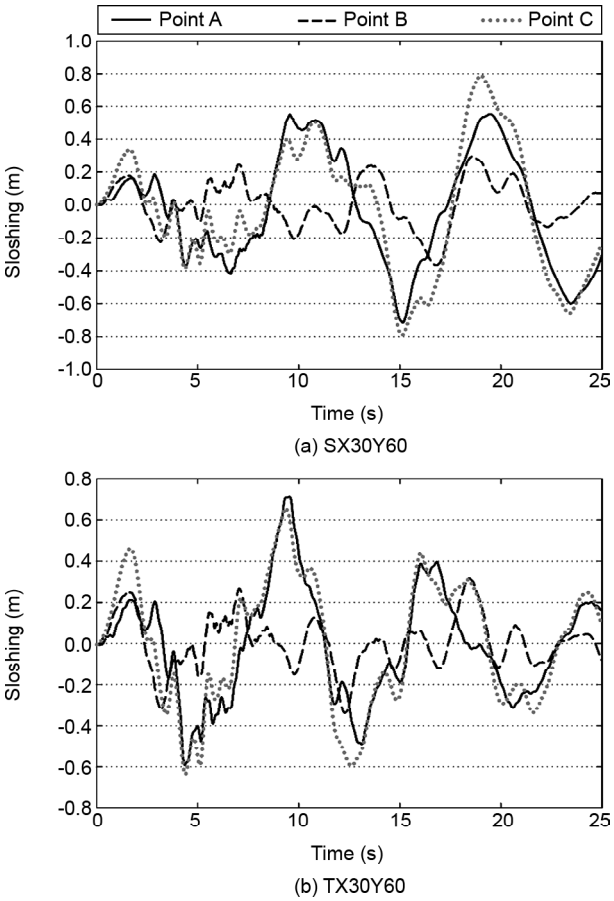

Figure 8. Time history of sloshing height under Loma791 record.

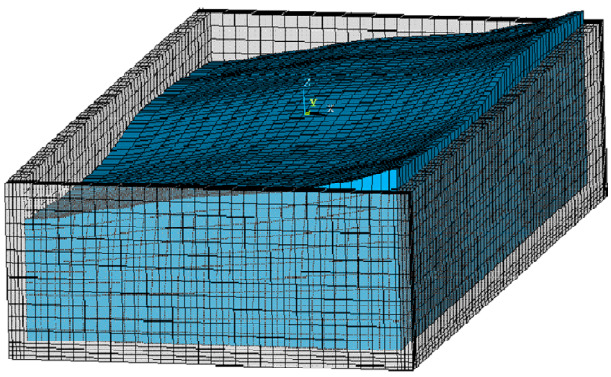

Figure 9. Free surface water change at corner TX30Y60 tank under Loma791 earthquake.

In Figure (10), sloshing height has been shown at Points A, B and C corresponding to the models of SX30Y60 and TX30Y60 under Loma745 earthquake. In SX30Y60 model, the maximum sloshing height at point C occurred in 15.56 sec. of analysis, equal to 13.9 cm. At this time, sloshing height at points A and B are equal to 13.4 and 0.1 cm, respectively. This issue indicates that the sloshing height in the tank corner and at point A has almost the same value. At this time, the sloshing height of the fluid is approximately the same as in all the wall faces, noting that the other component of earthquake record has little effect on the responses. Besides, the maximum negative sloshing height at point C has been obtained at 21.42 sec. equal to 17.1 cm. At this time, the maximum sloshing height at points A and B have been determined equal to 8.2 and 9.0 cm, respectively. The sloshing height at point C showed a larger value up to 101 percent and 90 percent compared to points A and B respectively.

In Figure (10-b), the maximum sloshing height at point A has been occurred at time 4.88 sec. equal to 20.3 cm while the sloshing height have been

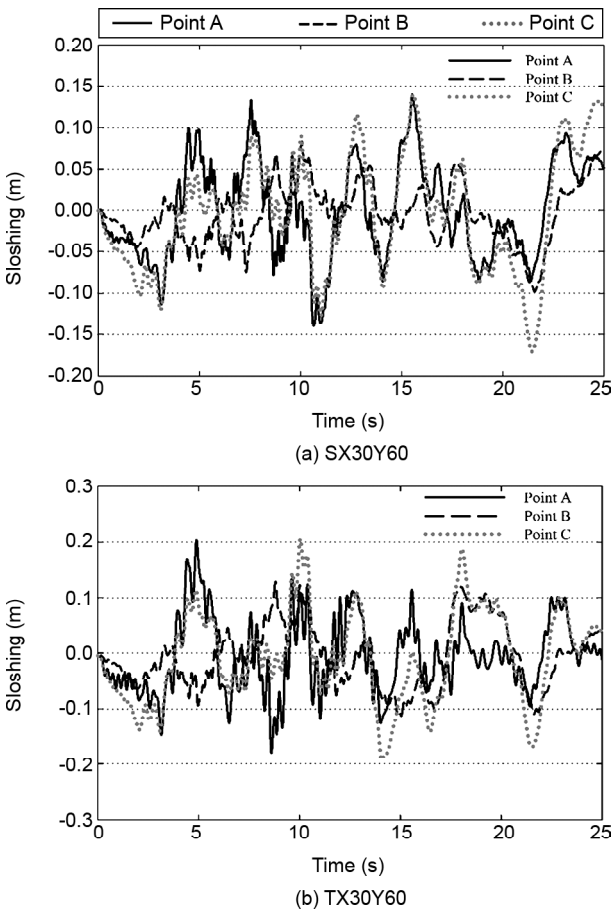

Figure 10. Time history of sloshing height under Loma745 record.

obtained equal to 5.8 and 11.2 cm at points B and C, respectively. On the other hand, the maximum sloshing height at point C has been occurred at time 10.04 sec. of analysis with the value of 20.6 cm, which showed up to 89 and 72 percent larger value compared to points A and B.

In Figure (11), variation of the sloshing height have been shown for Points A, B and C corresponding to models SX30Y60 and TX30Y60 under San Fernando91 earthquake. In the model SX30Y60, the maximum positive sloshing height has been occurred at point B and at time 8.46 sec. of the analysis equal to 4.8 cm. At this time, sloshing height has been obtained at points A and C equal to 1.2 and 3.0 cm. At time 7.70 sec. of the analysis, the maximum sloshing height has been occurred at point C and equal to 5.6 cm. At this time, corresponding height at points A and B reached to 4.3 and 2.5 cm, which present a larger value up to 30 and 124 percent compared to points A and B.

In Figure (11b), the maximum negative sloshing height has been occurred at point A at time 3.76 sec.

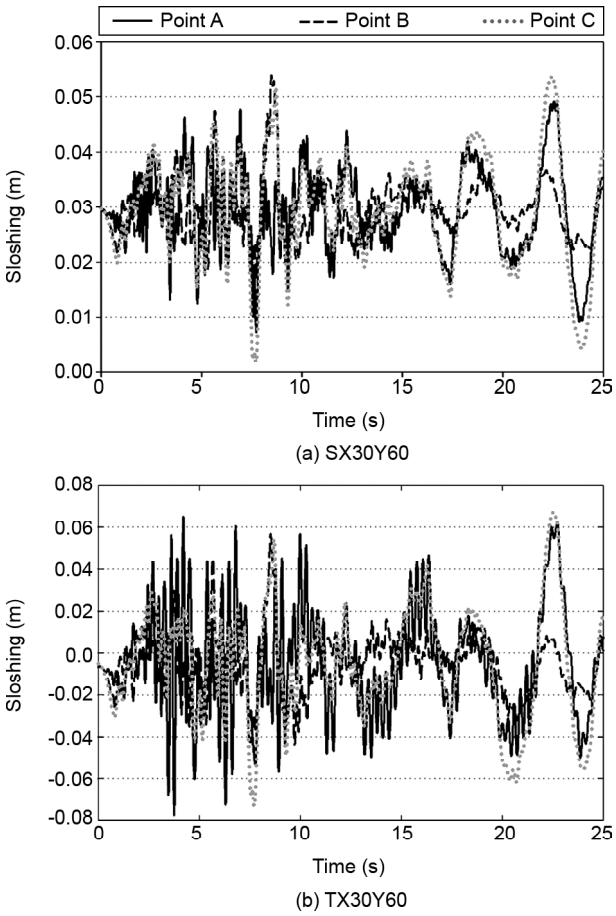

Figure 11. Time history of sloshing height under San Fernando91 record.

of the analysis equal to 7.7 cm. The corresponding height at points B and C have been obtained equal to 3 and 1.3 cm, respectively. On the other hand, the maximum positive sloshing height at point C has been occurred at time 22.50 sec. of the analysis. At this time, sloshing height at points A, B and C has been determined equal to 5.7, 0.6 and 6.7 cm, respectively. It should be noted that the sloshing height at point C is up to 17.5 percent greater than point A. As the obtained results show, seismic inputs with low and high frequency content caused the maximum and minimum height of sloshing, respectively. Accordingly, type of seismic input affect significantly the response of tanks. In addition, maximum height of sloshing in the corner of the tank can be several times the height of sloshing height in the middle of the tank. On the other hand, it is dependent to ratio dimension of plan tank and height of the water in tank.

5. Concluding Remarks

This paper discussed about the fluid-structure interaction using finite element method to obtain the effect of three-dimensional sloshing in rectangular concrete tanks under different earthquakes with various characteristics. However, it was shown that the hydrodynamic pressure value and its distribution is very sensitive to wall flexibility especially for seismic inputs with high frequency content.

The results showed that seismic inputs with lower frequency content results in higher sloshing wave height due to the smaller difference between the governing sloshing frequencies with the mass center of the power amplitude function of the earthquake. The sloshing height showed to be very sensitive and related to the ratio of tank dimensions to the height of water content.

The interaction analysis on the three-dimensional models showed that the combined sloshing height due to the longitudinal and transversal wave interference at the corners of the rectangular tank can be much higher than the wave height at the middle points of the wall in each direction. The less the difference between the sloshing frequencies for the two directions, the more the probability of the formation of the combined wave with maximum amplitude will be. This amplitude depends on the

ratio of the tank dimensions. The analyses showed that if the ratio of the tank dimensions approaches to unity, the maximum combined wave height could be formed.

The results has also showed that although the sloshing wave height increases at the corners due to the combination effect in three dimensions, the hydrodynamic pressure value decreases with a totally different distribution compared to the mid span zone of the walls. All these aforementioned effects have not been considered in the existing guidelines for tank design.

Acknowledgements

The support by the department of Civil, Water and Environmental Engineering of Shahid Beheshti University, Shahid Abbaspour Campus is gratefully appreciated.

References

1. Haroun, M.A. (1983) Vibration studies and tests of liquid storage tanks. *Earthquake Engineering and Structural Dynamics*, **11**, 179-206.
2. Hoskins, L.M. and Jacobsen, L.S. (1934) Water pressure in a tank caused by a simulated earthquake. *Bulletin of the Seismological Society of America*, **24**, 1-32.
3. Graham, E.W. and Rodriquez, A.M. (1951) *The Characteristics of Fuel Motion which Affect Airplane Dynamics. Douglas Aircraft Co. Inc. Santa Monica*.
4. Housner, G.W. (1963) The dynamic behavior of water tanks. *Bulletin of Seismological Society of America*, **53**, 381-387.
5. Housner, G.W. (1957) Dynamic pressures on accelerated fluid containers. *Bulletin of the Seismological Society of America*, **47**, 15-35.
6. ACI 350.3-06 (2006) *Seismic Design of Liquid-Containing Concrete Structures and Commentary*. American Concrete Institude (ACI) Committee 350.
7. Epstein, H.I. (1976) Seismic design of liquid-storage tanks. *Journal of the Structural Division*, **102**, 1659-1673.
8. Haroun, M.A. (1984) Stress analysis of rectangular walls under seismicity induced hydrodynamic loads. *Bulletin of the Seismological Society of America*, **74**, 1031-1041.
9. Kim, J.K., Koh, H.M., and Kwahk, I.J. (1996) Dynamic response of rectangular flexible fluid containers. *Journal of Engineering Mechanics*, **122**, 807-817.
10. Dogangün, A., Durmus, A., and Ayvaz, Y. (1997) Earthquake analysis of flexible rectangular tanks by using the Lagrangian fluid finite element. *European Journal of Mechanics*, **16**, 165-182.
11. Koh, H.M., Kim, J.K., and Park, J.H. (1998) Fluid-structure interaction analysis of 3-D rectangular tanks by a variationally coupled BEM-FEM and comparison with test results. *Earthquake Engineering and Structural Dynamics*, **27**, 109-124.
12. Chen, J.Z. and Kianoush, M.R. (2005) Seismic response of concrete rectangular tanks for liquid containing structures. *Journal of Civil Engineering*, **32**, 739-752.
13. Kianoush, M.R. and Chen, J.Z. (2006) Effect of vertical acceleration on response of concrete rectangular liquid storage tanks. *Engineering Structures*, **28**, 704-715.
14. Kianoush, M.R., Mirzabozorg, H., and Ghaemian, M. (2006) Dynamic analysis of rectangular liquid containers in three-dimensional space. *Journal of Civil Engineering*, **33**, 501-507.
15. Livaoglu, R. (2008) Investigation of seismic behavior of fluid-rectangular tank-soil/foundation systems in frequency domain. *Soil Dynamics and Earthquake Engineering*, **28**, 132-146.
16. Hosseini, M. and Abizadeh, S. (2013) Behavior of reinforced concrete rectangular aboveground tanks subjected to near-source seismic excitations. *American Environmentalism: Philosophy, History, and Public Policy*, 449-454.
17. Hosseini, M., Vosoughifar, H., and Farshadmanesh, P. (2013) Simplified dynamic analysis of sloshing in rectangular tanks with multiple vertical baffles. *Journal of Water Sciences Research*, **5**, 19-30.

18. Ghaemmaghami, A.R. and Kianoush, M.R. (2010) Effect of wall flexibility on dynamic response of concrete rectangular liquid storage tanks under horizontal and vertical ground motions. *Journal of Structural Engineering*, **136**, 441-451.

19. Federal Emergency Management Agency (2009) *Quantification of Building Seismic Performance Factors*. Report no. FEMA P695, FEMA, Washington, DC.

20. Hashemi, S., Saadatpour, M.M., and Kianoush, M.R. (2013) Dynamic behavior of flexible rectangular fluid containers. *Thin Walled Structures*, **66**, 23-38.